Chapter 4

Analysis of the mixing efficiency in rotors design

To explain how our dispersive models can be used to analyze mixing efficiency of different batch mixers, let us now compare dispersive mixing efficiency of two existing tangential rotors respectively called : ZZ2 rotor and Old-Standard rotor (Figure 4.1). Distributive mixing efficiency of these rotors is also evaluated to obtain a global vision of their mixing performance.

4.1 Flow in batch mixer

Large number of contributions in literature demonstrate that numerical simulation is a useful tool to evaluate mixing efficiency of devices as twin-screw extruder or batch mixers. Different one-dimensional and bidimensional models have been proposed (Booy,1980) (Lozano et al,2002) (Szydlowski et al,1987) (Speur et al,1987) (Potente et al,1997). But, we have to perform three dimensional time dependent calculation to catch all information on the flow generated by these rotors. Flow pattern generated by each couple of rotor in mixer chamber is calculated with constrained finite element formulation for non-conforming meshes.

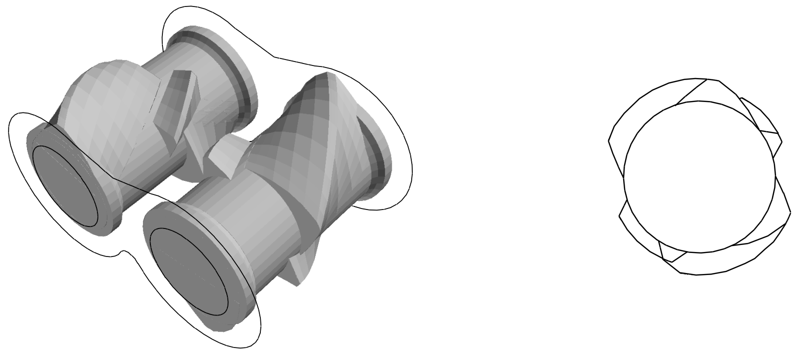

(a) 3D view and front view of Old-Standard rotor

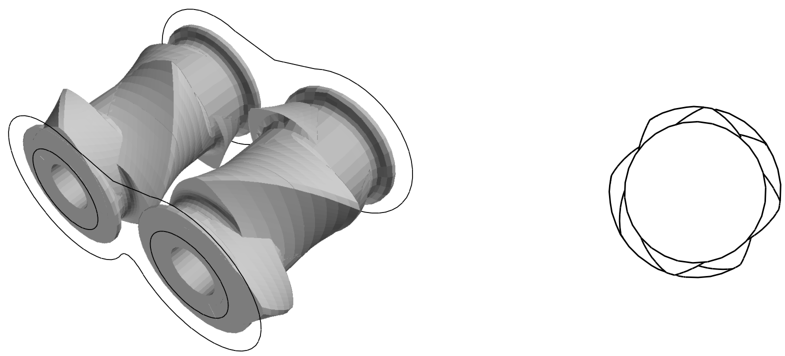

(b) 3D view and front view of ZZ2 rotor

Figure 4.1: Two kinds of four wings rotor are compared : (a) Old-Standard rotor and (b) ZZ2 rotor.

Firstly, we recall the governing partial differential equation of isothermal and incompressible flow of generalized Newtonian fluid:

$$\begin{cases} \rho \, \dfrac{D\mathbf{v}}{Dt} = -\nabla p + \nabla \cdot \tau + \rho \, \mathbf{g} \\ \nabla \cdot \mathbf{v} = 0 \end{cases} \tag{4.1}$$

where D/Dt is the material derivative, $\mathbf{v}$ is the velocity, p is the pressure, ρ is the density, $\mathbf{g}$ is the gravity and τ is the extra-stress tensor defined by:

$$\tau = 2\eta(\dot{\gamma})\mathbf{d}$$

with the strain rate tensor $\mathbf{d}$ and the kinematic viscosity η. Shear rate $\dot{\gamma}$ is defined as the square root of the second invariant of strain rate tensor,

$$\dot{\gamma} = \sqrt{2\mathbf{d}:\mathbf{d}}$$

As we consider flows in a batch mixer with a rotational speed of 30 rpm, we are dealing with $Re \sim 10^{-5}$ and $Re/Fr \sim 10^{-3}$. In other words, we consider creeping flow assumption and neglect gravity effects.

To build a mathematical model of rubber mixing process in batch mixer, several geometrical assumptions and simplified constitutive model for the fluid are selected (Meijer,1997). Correct balance between the complexity of the geometrical model and the complexity of the rheological model has to be identified. The use of complex rheological model with relatively coarse geometrical discretization is not relevant as to consider irrelevant geometrical details with very poor rheological model. Suitable compromise between numerical and modeling errors has to be determined in taking into account the cost of large time-dependent three-dimensional calculation and the numerical accuracy that can be obtained. In view of the geometrical assumptions that we have to introduce, it seems reasonable to reproduce only the shear thinning behavior of the mix rubber-carbon black by Bird-Carreau model (Barnes et al,1989) (Macosko et al,1994) :

$$\eta(\dot{\gamma}) = \eta_\infty + (\eta_0 - \eta_\infty)\left(1 + (\lambda\dot{\gamma})^2\right)^{(n-1)/2} \tag{4.2}$$

where $\eta_0 = 1\,10^6\,Pa\,s$ is the zero shear rate viscosity, $\lambda = 10\,s$ is a natural time, $\eta_\infty = 10\,Pa\,s$ is the infinite shear rate viscosity and $n = 0.23$ is the power law index. Those parameters have been selected to fit the experimental measurements at a temperature of $140°C$ of a reference mix rubber-carbon black used by Michelin. Density of this mix is equal to $1066\,kg/m^3$.

In a first approach, we consider that the flow is isothermal and we impose full sticking condition along the wall of the mixer chamber and along the rotors. Obviously, these

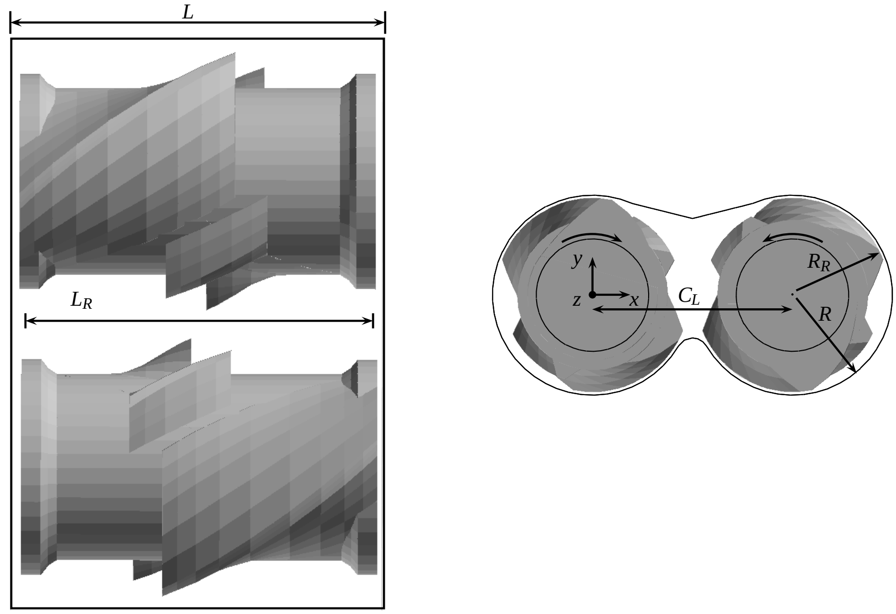

Figure 4.2: Geometrical parameters that define the shape of the rotors and the mixer chamber.

are two strong assumptions. In such a mixing process, flow is often non-isothermal but sometimes thermal regulation is adjusted to obtain an isothermal flow during a short period of time. In other words, we here assume that we are in this specific condition. With this assumption, we obtain a periodic flow pattern after only one revolution of the rotors. We can then calculate the evolution of the mixing on more than one revolution by repeating several time this flow pattern. Most people observe partial slipping of rubber along the rotors and the mixer chamber. As the amount of the slipping along the mixer chamber is still an open question deserving a full analysis, it seems to be fair to restrict ourselves to a stick condition. Finally, the mixer chamber is assumed to be fully-filled because numerical simulation of a partially filled domain requires both extremely sophisticated algorithms and prohibitive cost.

The two rotors (ZZ2 and Old-Standard) have a counter-rotating motion at 30 rpm in the mixer chamber. Material is introduced by the top of the mixer chamber and is pushed to the bottom of the mixer by the rotors. In the same time, material is distributed in the whole volume of the mixer chamber. Old-Standard rotors is composed of two short and two long wings that are respectively located in the middle of the rotor and at the extremeties of the rotors. ZZ2 rotor is also composed of two long wings and two small wings, but long wings are located in the middle of the rotor and small wings are located at the extremities of the rotor. Typical dimensions of these rotors and dimensions of the mixer chamber are given in Table 4.1 and illustrated in Figure 4.2.

Mixer chamber dimensions (mm)		
Length L	208	
Radius R	80	
Centerline C_L	160	
Rotors dimensions (mm)		
	ZZ2	Old-Standard
Length L_R	198	198
Radius R_R	78.5	78.25
Clearance size	1.5	1.75
Fluid volume (dm^3)		
ZZ2	3.5	
Old-Standard	3.9	

Table 4.1: Dimensions of the mixer chamber, of the ZZ2 rotors and of the Old-Standard rotors.

4.2 FEM flow calculation

To calculate the flow pattern generated by the motion of the rotors in the mixer chamber, we use a finite element software dedicated to highly viscous flows: POLYFLOW (Debbaut et al,1991). In order to get reliable results, a fine design of the mesh and a suitable selection of the mixed interpolations remain critical.

Time dependent fields can be calculated with different techniques. In 2000, Yoshinaga and Ishikiwa et al. performed three-dimensional time-dependent simulation of the mixing in twin-screw extruders by generating a new mesh for each position of the screws at each time step. Interpolation between meshes allows obtaining the time dependent fields. Unfortunately, this simple technique is very time consuming. Rios et al. (2000) have proposed to use boundary element method to perform such a simulation. This technique offers an alternative to the meshing effort but incorporating non-linearity of rheological model is a very tedious issue. In our work, we use a penalty technique that allows us to avoid the complex task of meshing the flow domain. Flow domain is the volume of the mixer chamber that is not filled by rotors. In this so-called *mesh superposition technique* (Avalosse et al,2000), we independently build the mesh of the mixer chamber and the mesh of each rotor. Meshes of the mixer chamber and the rotors are then superimposed as illustrated in Figure 4.3. Position of the rotors is automatically updated at each time step. For each node of the mixer chamber mesh, we have to detect if node is included in one of both rotors or in actual "fluid" region. Outside the rotors, the velocity of the node is calculated by satisfying the weak formulation of Navier-Stokes equations. Otherwise the velocity of the node is constrained at the rotors velocity. This technique can be directly compared to the *fictitious domain method* used by Bertrand et al. They impose kinematic constrains by means of Lagrange multipliers and not by a penalty technique.

Mesh superposition technique presents two major advantages. Firstly, only two meshes without complex intermeshing regions have to be built to perform a transient simulation. Secondly, the method is efficient and robust thanks to the absence of remeshing algorithm. Nevertheless, the accuracy of this method is lower than the accuracy of a classical method and requires a mesh refinement. Obviously, if the mesh becomes too coarse in some areas, very poor numerical results can be obtained. Typically, mass conservation cannot be always guaranteed; fluid leakage can appear in some critical parts of the flow domain. Such a bad behavior comes from the penalty formulation used in the mesh superposition technique that is not formally a conservative numerical technique: we have thus to maintain mass conservation under control. The local mass loss can modify in a significant way the flow features and therefore the quality of the mixing analysis.

In previous work, we studied the mixing efficiency of twin-screw extruders with the same technique (Alsteens et al,2005) and we determined guidelines to build an efficient mesh for such simulations. High shear rates, that imply a decreasing of viscosity, are usually observed in clearance zones (zones between the tip of the wings of the rotors and the wall of the mixer chamber). Such an effect is only captured if the mesh is at least composed of three bricks in these zones. Otherwise, the variation of velocity field due to the decreasing of shear rate is not observed. In order to obtain accurate evolution of flow pattern in time, we divide one rotation of the rotor in 45 time steps. Rotors then rotate of 8° at each time step. But small time steps are useless if the circumference of each mixer chamber is not divided in a minimum of 45 segments. If the size of these segments is too large, the rotors motion will not be accurately detected with mesh superposition technique. Finally, the mesh has to be refined in radial and axial directions at proximity of the wall of the mixer chamber to capture the shear rate evolution in these zones. From these guidelines, a mesh that is a good

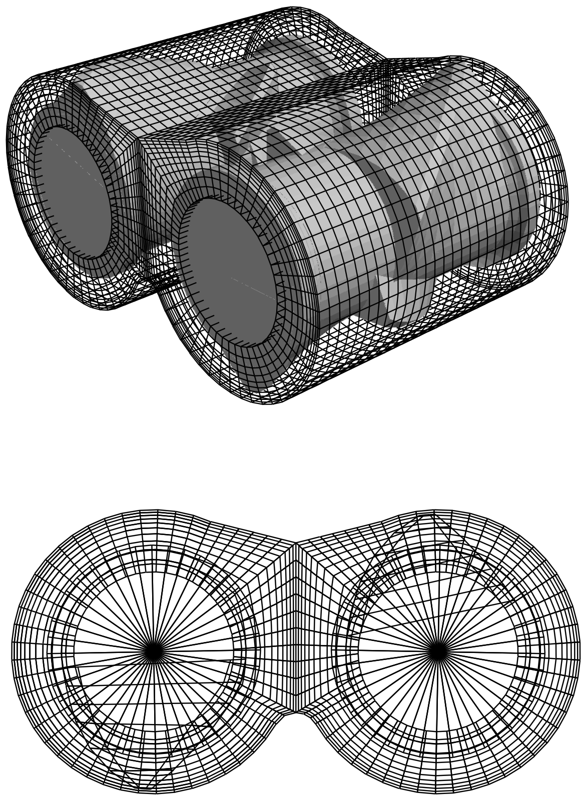

Figure 4.3: Superposition of the meshes of the mixer chamber and the rotors.

compromise between the number of degrees of freedom and the required accuracy has been built. Number of bricks in the different directions are given in Table 4.2. This mesh is composed of 34.508 bricks.

For Stokes problem, it is well known that the interpolation of velocity and pressure has to satisfy the Brezzi-Babuska condition (Brezzi et al,1991) for a usual Galerkin formulation as used in the software. Otherwise, a stabilized pressure Petrov Galerkin formulation could be used with an equal-order approximation. Moreover, in our specific application, penalty technique applied on flow bricks partially superimposed by rotors, requires special care because locally the ratio between velocities and pressure unknowns is modified in the wrong way for stability issue. We can choose between

Mesh refinement of the mixer chamber		
Circumference	Axial direction	Radial direction
46	28	10

Table 4.2: Mesh refinement along the circumference of the mixer chamber and in the axial and radial directions.

three mixed interpolations defined in Figure 4.4.

- $Q_1 - Q_0$: hexahedral linear velocity and constant pressure interpolation. Such an element is widely used in a large number of applications even if it does not formally satisfy the Brezzi-Babuska condition.

- $Q_1^+ - Q_0$: mini-element velocity and constant pressure interpolation. Velocity interpolation is a usual hexahedral linear element at which a scalar degree of freedom is added in each face.

- $Q_1^{++} - Q_1$: enriched mini-element velocity and linear pressure interpolation. An additional bubble function enriches the velocity field to define Q_1^{++} element from Q_1^+ element.

Choice of the relevant interpolation is a tedious task. In the paper on the mixing efficiency of twin-screw extruder (Alsteens et al,2005), we have studied the effect of these interpolations on pressure profile along the extruder. It appears that $Q_1^{++} - Q_1$ and $Q_1^+ - Q_0$ interpolations provide similar results, but some local spurious oscillations have been observed in pressure profile obtained with $Q_1^{++} - Q_1$. $Q_1 - Q_0$ element underestimates the pressure drop. Best compromise between numerical cost and accuracy was to be addressed by the $Q_1^+ - Q_0$ element for a given mesh in these simulations. But present simulations are most expensive and we are limited to use $Q_1 - Q_0$ interpolation. The cost of such a simulation with the mesh described in Table 4.2 remains important. Transient simulation takes around 12 days for 45 times steps and requires 1578 Mbytes of memory on a DEC Alpha server (600Mhz-1Gb of memory) when the power law index of Bird-Carreau law is equal to 0.23.

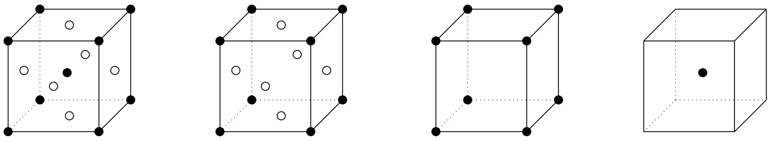

Figure 4.4: Enriched mini-element (Q_1^{++}), mini-element (Q_1^+), linear element (Q_1) and constant element (Q_0). Black dots mean that all components of a vector field are considered as degree of freedom. White dots mean that only a normal scalar degree of freedom is defined for the considered field.

4.3 Comparison of the mixing efficiency of ZZ2 and Old-Standard rotors.

Calculation of flow pattern in the mixer chamber shows that counter-rotating motion of the rotors drags the fluid from ram door to drop door in circumferential motion. If the drop door is closed, the fluid flows in right and left regions of the mixer and comes back progressively to the top of the mixer as illustrated in Figure 4.5.

In the same time, the fluid moves in the mixer along the z-axis due to the wings shape. This axial motion of the fluid is totally different with ZZ2 and Old-Standard rotors. We show in Figure 4.6 and Figure 4.7 the evolution of axial velocity v_z in a horizontal plane located in the middle of the mixer chamber for Old-Standard and ZZ2 rotors respectively.

This evolution allows us to distinguish two kinds of axial flow as illustrated in Figure 4.8. With Old-Standard rotor, the fluid is dragged from the front to the back of the mixer chamber along right rotor and from the back to the front of the mixer chamber along left rotor during the first quarter of revolution. Moreover the axial velocity v_z is very small in the middle of the chamber, but a transfer of fluid between both rotors is observed. With ZZ2 rotors, the fluid flows from the front to the back of the chamber in the middle of the mixer and the fluid is dragged from the back to the front of the mixer along left and right rotors. As for Old-Standard rotors, a transfer of fluid is observed

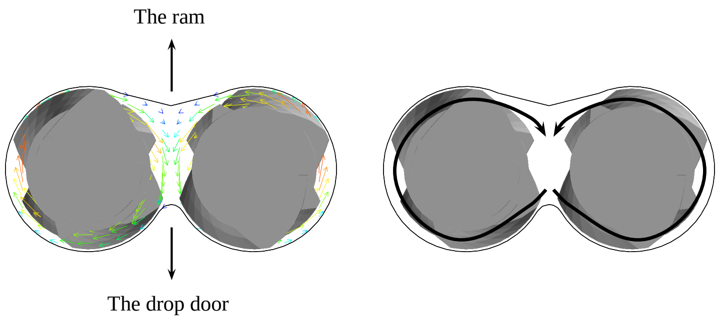

Figure 4.5: Counter-rotating motion of ZZ2 and Old-Standard rotors gives a rotational motion to the fluid.

between both rotors. In the third quarter of revolution, ZZ2 and Old-Standard rotors generate respectively the same kind of flows than in the first quarter of revolution but reversed. A period of transition is finally observed in second and fourth quarter of revolution. Let us now evaluate the distributive mixing efficency of these flows.

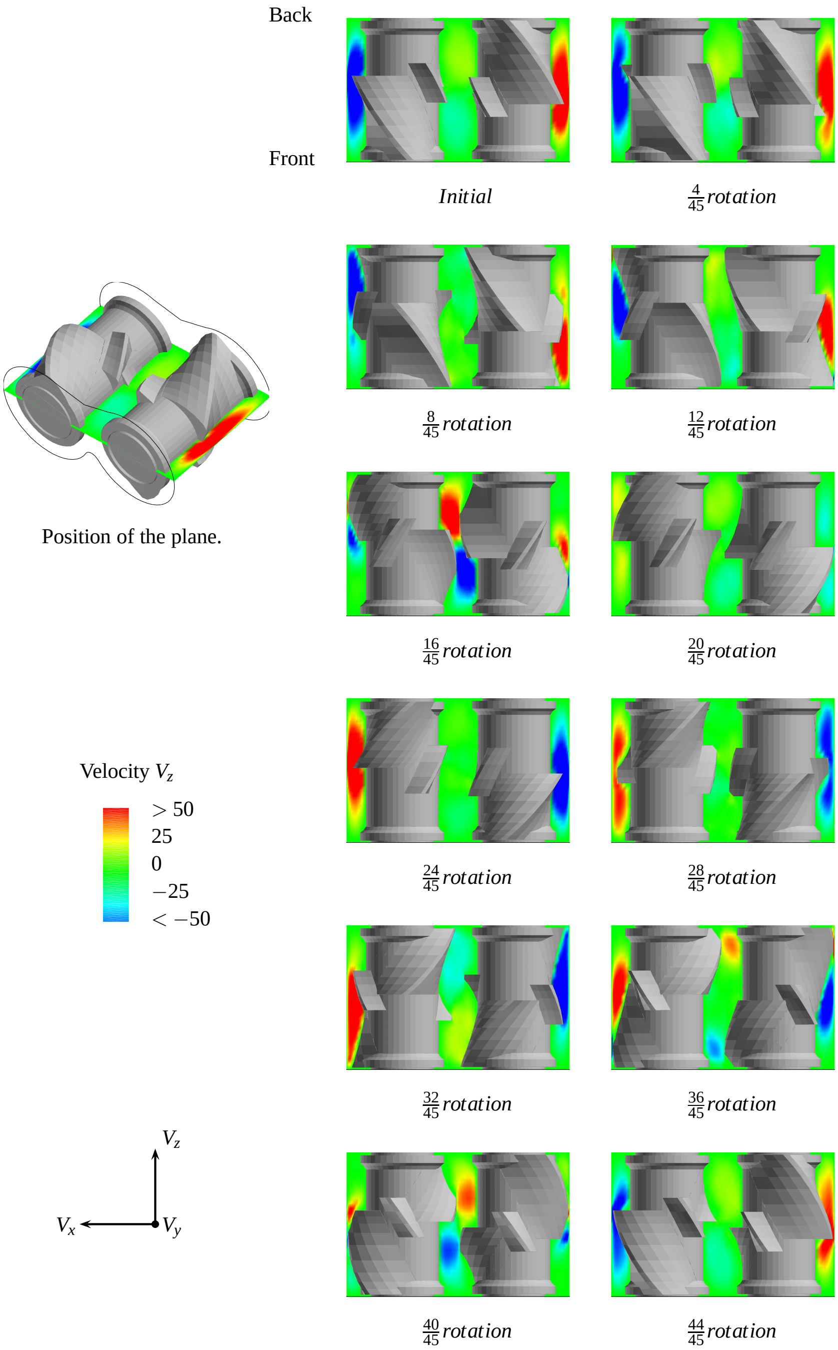

Figure 4.6: Evolution of axial velocity v_z during one revolution of Old-Standard rotors in a horizontal plane located in the middle of the mixer.

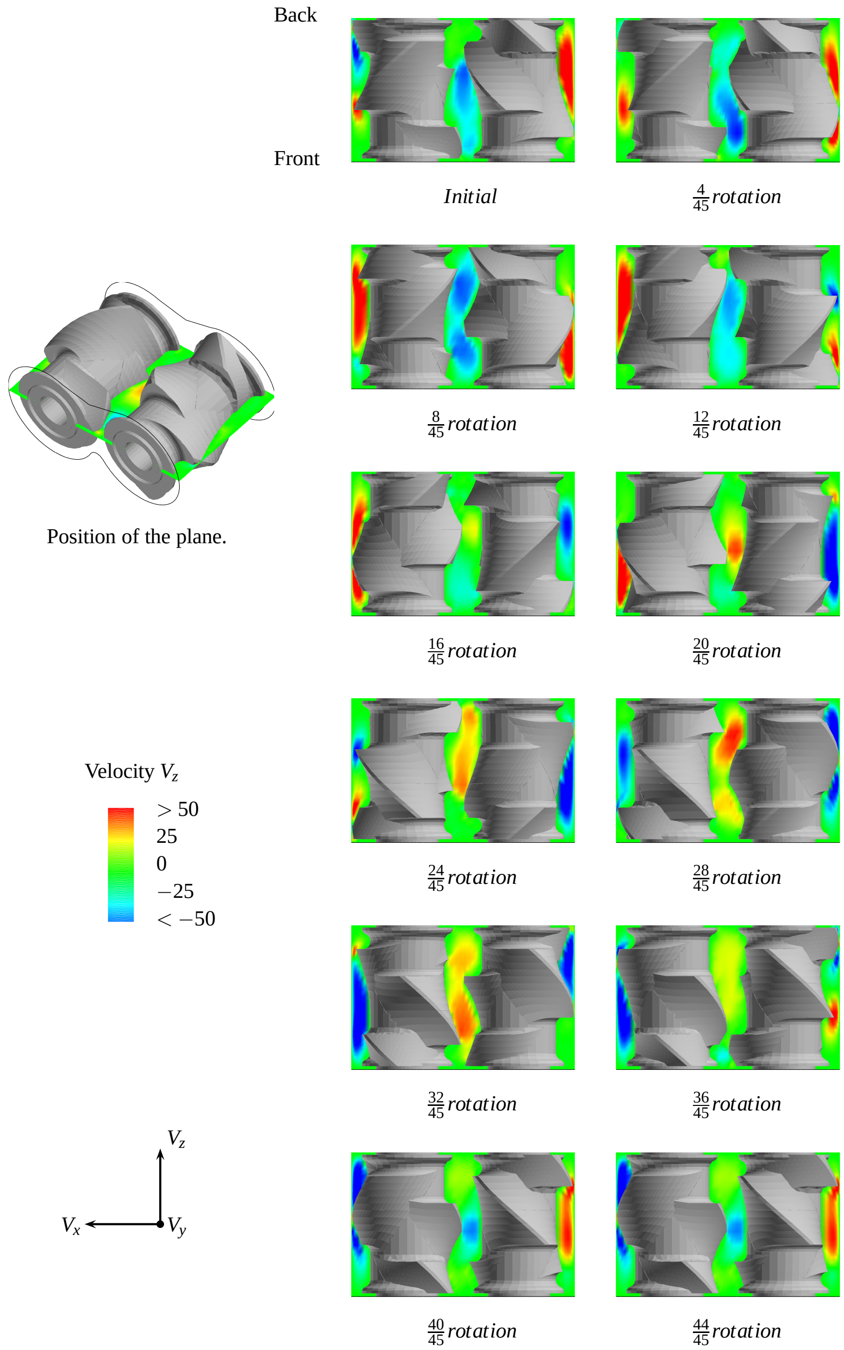

Figure 4.7: Evolution of axial velocity v_z during one revolution of ZZ2 rotors in a horizontal plane located in the middle of the mixer.

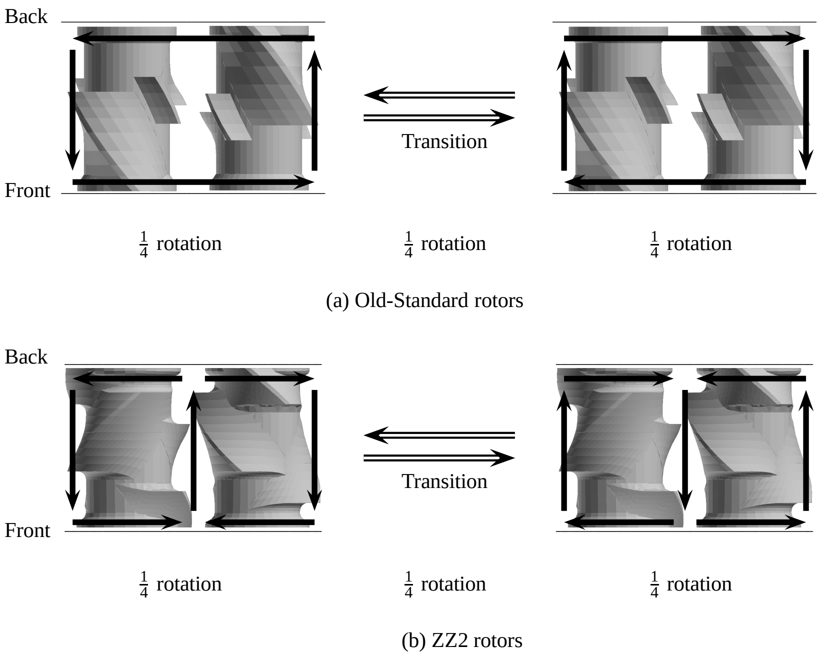

(a) Old-Standard rotors

(b) ZZ2 rotors

Figure 4.8: Axial flow generated by the motion of ZZ2 and Old-Standard rotors in the mixer chamber.

4.3.1 Distributive mixing efficiency

Distributive mixing efficiency of these rotors is evaluated by calculating during 20 seconds the trajectory of one thousand particles initially located in a small box ($40mm\,x\,40mm\,x\,40mm$) below the ram as illustrated in Figure 4.9. The distribution of these particles in mixer chamber is compared to an optimum distribution corresponding to a random distribution of one thousand particles in the whole flow domain. For any time t, we evaluate the frequency to find a pair of neighboring points distant from d in both distributions. These frequencies are respectively noted f_d and f_d^{opt} for the actual and the optimum distributions. The deviation between both distributions can be evaluated as following :

$$\delta_d(t) \ = \ \frac{1}{2}\int_0^\infty \left| f_d(t,l) - f_d^{opt}(l) \right| \ dl$$

Smaller this deviation, better the distributive mixing. This deviation is called distributive index.

We can observe in Figure 4.10 the evolution of the distributive index for both configurations. Material points distribution in the whole flow domain is slightly faster with ZZ2 rotors than with Old-Standard rotors. After 20 seconds of mixing, distributive index is equal to 0.12 and 0.23 for ZZ2 and Old-Standard rotors respectively. It seems therefore that ZZ2 rotors is most efficient than Old-Standard rotors to generate a good distributive mixing.

Let us now analyze the axial distribution of the material points in the flow domain. This distribution is calculated by collecting the axial coordinate of all particles at different times t. These material points are initially located in the same box than previously with a z-coordinates between $84mm$ and $124mm$. We can observe in Figure 4.11a and 4.11b the evolution in time of the axial distribution of the material points for Old-Standard and ZZ2 rotors. Solid red curve represents the axial distribution obtained after 20 seconds of mixing and black curves represent the evolution of the axial distribution from 0 second to 4 seconds. Distribution width increases progressively in time in both cases but the axial distribution obtained with Old-Standard rotors is always symetric. With ZZ2 rotors, the axial distribution moves on the left at the start of the mixing and is finally symetric after 20 seconds.

The comparison of these axial distributions with an optimum axial distribution, obtained by collecting the axial coordinate of all particles when they are randomly distributed in the whole flow domain, allows us to evaluate the efficiency of these rotors to axially distribute the particles. The dotted red curve represents this optimum axial

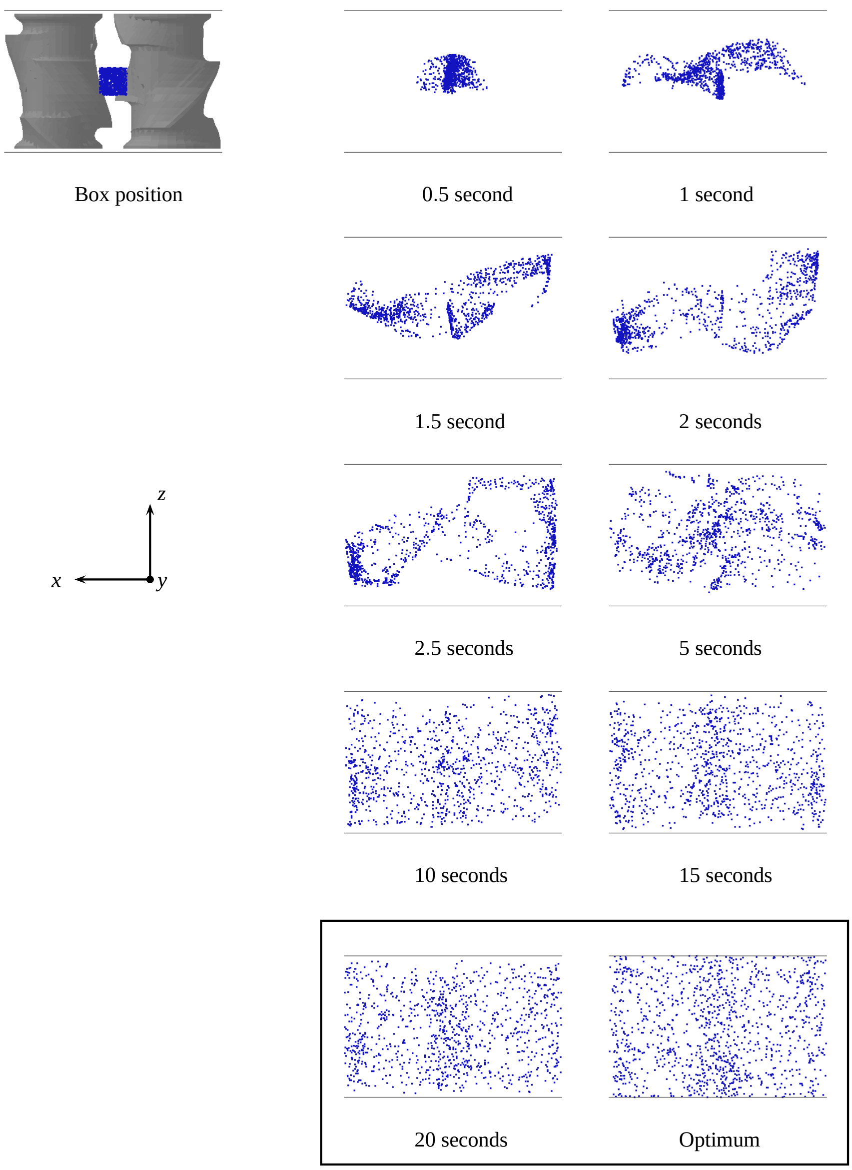

Figure 4.9: Distribution of one thousand particles in the mixer chamber with ZZ2 rotors.

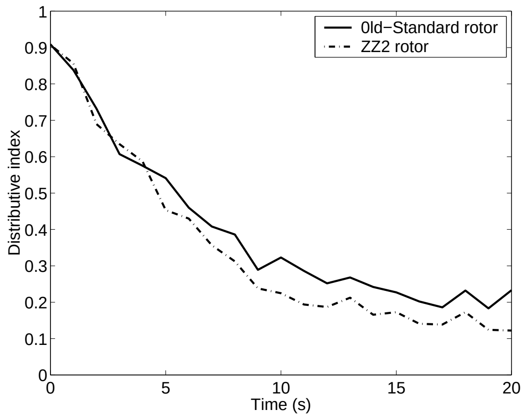

Figure 4.10: Evolution of the distributive index for Old-Standard and ZZ2 rotors versus the time of mixing.

distribution. The deviation between the optimum and actual distributions is given by

$$\delta_z(t) \ = \ \frac{1}{2}\int_0^\infty \left| f_z(t,z) - f_z^{opt}(z) \right| \ dz$$

where f_z and f_z^{opt} are the frequencies to find a particle in a given axial coordinate in the actual and optimum distribution respectively. The evolution of this deviation, illustrated in Figure 4.11c, shows that the axial distribution of the material points is faster with the ZZ2 rotors than with the Old-Standard rotors. But the difference between both curves reduces when the mixing time increases.

Finally, it is also important to observe a good transfer of the particles from one rotor to the other one. Let us imagine that we have initially white and blue components located respectively in the left and in the right parts of the mixer chamber. If the transfer between both parts is not efficient, we never reach a good level of distribution of the blue component in the white component. In order to quantify this transfer, we evaluate the percentage of particles of the optimum distribution, for any time t, that is exchanged between both rotors. Larger this number, better the transfer. We can observe in Table 4.3 that this transfer is more efficient with the Old-Standard rotors than with the ZZ2 rotors.

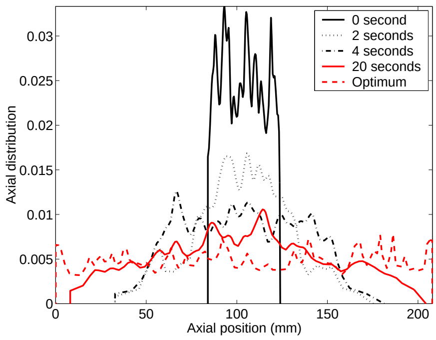

(a) Old-Standard rotor

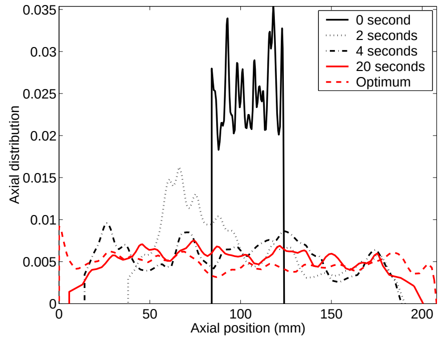

(b) ZZ2 rotor

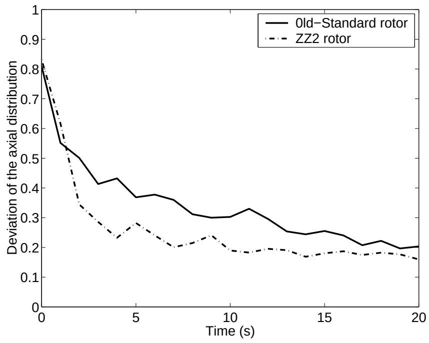

(c) Deviation $\delta_z(t)$

Figure 4.11: Evolution of the axial distribution of material points in the mixer chamber for ZZ2 and Old-Standard rotors and the evolution of the deviation $\delta_z(t)$ for both rotors.

4.3.2 Dispersive mixing efficiency

To evaluate the dispersive mixing efficiency of ZZ2 and Old-Standard rotors, we firstly estimate the shear rate distribution in the flow domain. As illustrated in Figure 4.12, the maximum shear rate is always observed in the gap between the top of the wings and the walls of the mixer chamber. The maximum of shear rate is upper than $80\,s^{-1}$ with each kind of rotor. Highest shear rates are observed in the clearance zones of the mixer with ZZ2 rotors due to the smaller gap observed in this mixer. Nevertheless, the histogram given in Figure 4.12 show us that the percentage of the whole fluid mass with a shear rate larger than $5\,s^{-1}$ is always higher in the flow generated with Old-Standard rotors than in the flow generated with ZZ2 rotors. We can therefore conclude

Rotors	Time (seconds)				
	0	5	10	15	20
Old-Standard	0%	42%	61%	71%	76%
ZZ2	0%	26%	44%	55%	62%

Table 4.3: Percentage of particles transfered between the left and the right parts of the mixer chamber in time.

that the flow generated by Old-Standard rotors is characterized by the highest shear rate outside the clearance zones. This difference on the shear rate evolution affects the dispersive mixing efficiency because the decreasing of the agglomerates size depends directly on the shear rate history.

We now compare the evolution of a given mass density distribution along the trajectory of five hundred particles randomly launched in the mixer with the ZZ2 rotors and with the Old-Standard rotors respectively. Each trajectory is calculated during 40 seconds. The initial mass density distribution is the initial mass distribution used in the numerical simulation of the Mooney experiments and is represented in blue in the following plots (Figure 4.13). Its evolution in time along each trajectory is calculated with the volume model where we assume that the parameter κ only depends on shear rate,

$$\kappa(\dot{\gamma}) = 1.2\,10^{-4}\,\dot{\gamma}$$

where $\dot{\gamma}$ is the shear rate measured along the trajectory and $1.2\,10^{-4}$ is the constant value that provides the best fit between the results obtained in the Mooney experiments at $2\,rpm$ ($\dot{\gamma} = 1$) and the numerical results.

We can observe in Figure 4.13a and Figure 4.13b that the mass density distributions obtained at the end of each trajectory with Old-Standard and ZZ2 rotors are quite similar. The number of mass density distributions that have a maximum of mass density lower than 0.07 or upper than 0.08 is almost identical with both rotors (Table 4.4). Nevertheless, only Old-Standard rotors provide two mass density distributions where all agglomerates have a size lower than $3\mu m$. These very small differences between the dispersive mixing efficiency of both rotors can be explained by studying the evolution of the shear rate along each trajectory in the mixer chamber.

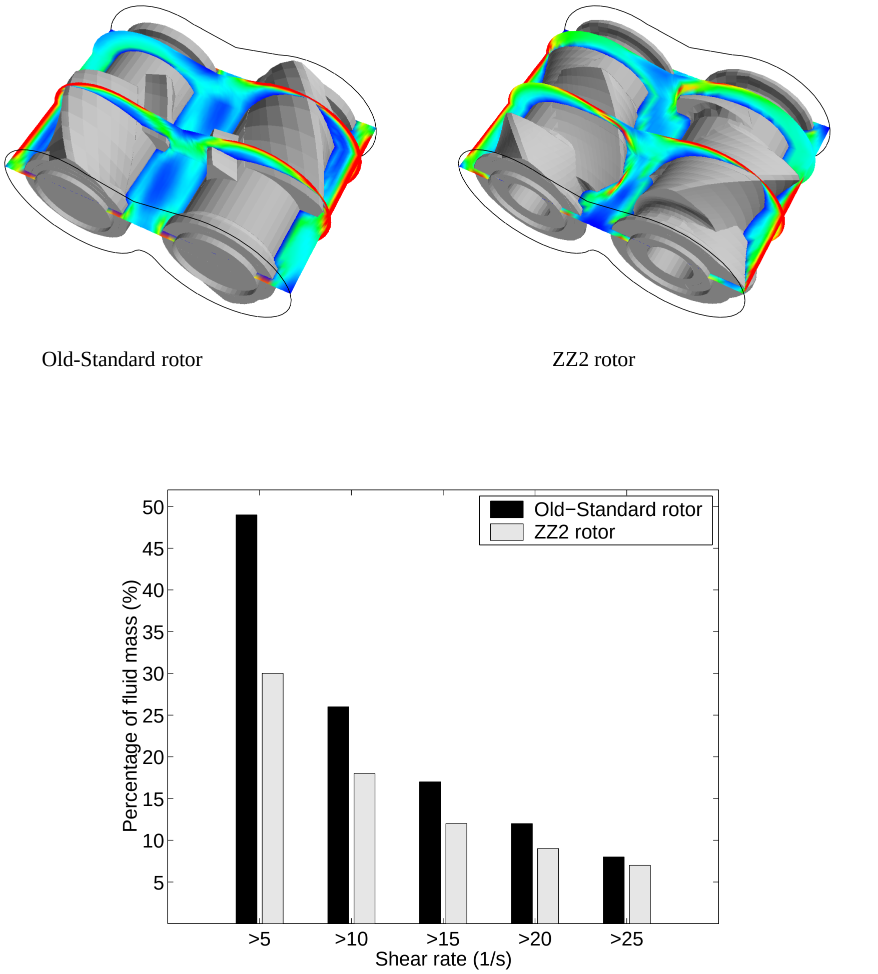

Figure 4.12: Shear rate field in the mixer and percentage of fluid mass with a shear rate larger than $5s^{-1}$, $10s^{-1}$, $15s^{-1}$, $20s^{-1}$ and $25s^{-1}$.

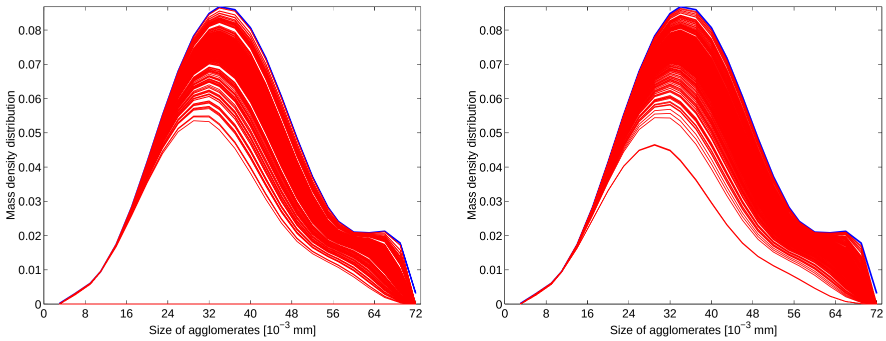

(a) Old-Standard rotors (b) ZZ2 rotors

Figure 4.13: Set of mass density distributions and mean density distributions obtained after 40 seconds of mixing with Old-Standard and ZZ2 rotors.

The same mass density distribution predicted by the dispersive model is obtained from different evolutions of shear rate so long as the integral of $\dot{\gamma}$ in time is kept constant. It is not only the instantaneous value of shear rate that is important but its integral in time along the whole trajectory. This integral is usually called *total shear*. This property of our models explains that we obtain the same results with the Old-Standard and with the ZZ2 rotors. We show in Figure 4.14a two evolutions of the shear rate that have provided the same mass density distribution with the ZZ2 and Old-Standard rotors. The high value of shear rate experienced one time by the particle with the Old-Standard rotor is compensated by several peaks at an intermediate value of the shear rate with the ZZ2 rotors. The distribution of the total shear obtained after 40 seconds of mixing are similar in both configurations as illustrated in Figure 4.14b.

With the Old-Standard rotors, the shear rate outside the clearance zones is higher than with the ZZ2 rotors, but the number of particles that cross the clearance zones is smaller. These high values of the shear rate experienced by the particles in the clearance zones with the ZZ2 rotors compensate the smaller value of the shear rate in the flow domain of this mixer. Let us now focus on the trajectories along which the shear rate is at least one time larger than $80s^{-1}$ with both rotors. These values of the shear rate are only observed in the clearance zones. We have respectively 210 and 244 trajectories with such a property in the flow generated by the ZZ2 and Old-Standard rotors respectively. But we can observe in Table 4.4 that the shear rate is more often greater than $80s^{-1}$ along the trajectories obtained with the ZZ2 rotors than with the Old-Standard rotors. This behavior tends to demonstrate that the particles cross more often the clearance zones with the ZZ2 rotors than with the Old-Standard rotors.

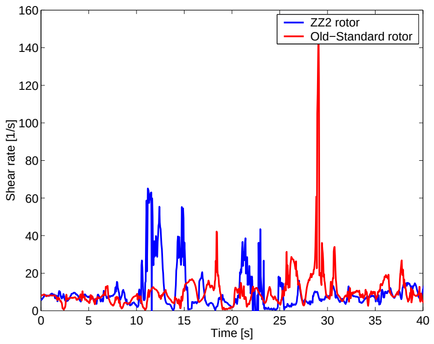

(a)

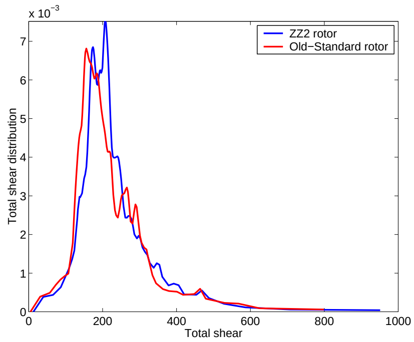

(b)

Figure 4.14: (a) Two evolutions of the shear rate that provides the same mass density distribution after 40 seconds and (b) the distributions of total shear obtained after 40 seconds of mixing obtained with the ZZ2 and Old-Standard rotors.

We finally conclude that the ZZ2 rotor is more efficient than the Old-Standard rotors to generate a good distributive and dispersive mixing. The evolution of the size of the agglomerates during the mixing is quite similar with both rotors, but the particles are better distributed throughout the flow domain with the ZZ2 rotors. Nevertheless, only the transfer of particles between the rotors is faster with the Old-Standard rotors than with the ZZ2 rotors. For an energetical point of view, it is important to note that the specific power required for the mixing is higher with the ZZ2 rotors than with the Old-Standard rotors. This can be due to the smallest clearance zones of the ZZ2 rotors.

Experimentally, Michelin and ThyssenKrupp ElastomerTechnic observe on their production site that the ZZ2 rotor is slightly more efficient to distribute the carbon black agglomerates in the rubber than the Old-Standard rotor. This is mainly due to the position of the long wings on the ZZ2 rotor that generate a more complex flow. The study on the distributive mixing efficiency of both rotors by the numerical approach provides the same results. We also observe that the distribution of the particles in the flow domain is faster with the ZZ2 rotor than with the Old-Standard rotor. For the dispersive mixing, the result is different. Experimentally, Michelin and ThyssenKrupp ElastomerTechnic observe that the position of the long wings on the Old-Standard rotor force the flow to cross the clearance zones at the top of the wings because the fluid is pushed on against the wall of the mixer chamber by those wings. The fluid cannot avoid the clearance zones by passing beside the wings as in the ZZ2 rotor. This effect is more important if the speed of the rotors is low and if the mixer chamber is partially-filled. In our simulation, the dispersive mixing efficiency of the ZZ2 rotor and the Old-Standard rotor are similar. This small deviation between experimental and numerical results might due to the assumptions performed in our simulations to calculate the flow field. We suppose that the flow is isothermal and that the mixer chamber is fully-filled. Both assumption modify the flow field and the amount of rubber that crosses the clearance zones might then be overestimated.

Property	Rotors	
	ZZ2	Old-Standard
Percentage of distribution with $\rho_{max} > 0.08$	8.4	7.8
Percentage of distribution with $0.08 > \rho_{max} > 0.07$	80.2	80.4
Percentage of distribution with $\rho_{max} < 0.07$	11.4	11.8
Percentage of trajectory with $\dot{\gamma}_{max} > 80\,s^{-1}$	42	48.8
Number of peaks of $\dot{\gamma}_{max} > 80\,s^{-1}$	3455	1529
Mean value of the total shear	239.8	226.8
Power (W)	8325	8187
Mean torque (Nm)	2650	2606
Specific power (kW/m^3)	2378.6	2099.2

Table 4.4: Characteristic values for both configurations after 40 seconds of mixing.

Conclusion

In this thesis, a model that predicts the size evolution of the carbon black agglomerates during their mixing in rubber matrix is built. The quality of this model is evaluated against experimental results. Finally, this model is used to evaluate the dispersive mixing efficiency of two present batch mixers.

The literature on the mechanism of dispersion explains that the dispersion of carbon black is mainly governed by two mechanisms : erosion and rupture. Erosion is a continuous mechanism that draws some tiny fragments from the surface of the agglomerate. Several kinetics laws are proposed to predict the evolution of a single agglomerate as a function of both shear rate and hydrodynamics forces acting on the agglomerates. The variation of agglomerate size r in time obeys to a power law in r. Rupture is a discontinuous mechanism that breaks up the agglomerate in two or more fragments of various sizes. The mechanism of rupture only occurs if the shear stress acting on the agglomerate exceeds a threshold value inversely proportional to the agglomerate size. Even if rupture is often considered as an instantaneous mechanism, the break-up of one agglomerate seems to require a characteristic rupture time. The number of fragments obtained after several ruptures is also a function of the time required to observe one rupture. Both mechanisms depend on the structure of the carbon black and on its porosity. The infiltration by the rubber matrix modifies the cohesion of the agglomerate and therefore its dispersion. The infiltration mechanism reinforces the agglomerate only if the depth at which the matrix is infiltrated in the agglomerate is larger than the depth at which the shear rate field is transmitted within the agglomerate. This effect is neglected in this work because the typical time of impregnation is very large with respect to the erosion speed and the critical time of rupture.

As the number of agglomerates in a mix rubber-carbon black is very high, it is unimaginable to calculate the evolution of the size of each agglomerate separately. A set of agglomerates located in a small representative volume centered in x is therefore approximated by the mass density distribution associated with these agglomerates by using the typical continuum assumption for the agglomerates. Three separation scales are identified accordingly to the continuum assumption : the agglomerate scale (lower than $10^{-2}\,mm$), the macroscopical scale (typically $10\,mm$) and an intermediate scale where the size of the agglomerates can be viewed as a continuum field. A phenomenological model that estimates the evolution of the mass density distribution with time is built. This model takes into account both mechanisms of dispersion. The transfer rate of mass density from a given size r to a set of other sizes s of agglomerates is calculated from a transfer function. This transfer function becomes a transfer matrix when we discretize the size interval of the agglomerates into several subintervals. Each entry of this matrix is the transfer rate of mass density from class i to class j. The major drawback of this appraoch is the large flexibility allowed in the design of the transfer function. If we increase the number of classes, we have a model with a very large number of parameters and it will be quite difficult to have experimental data to identify these parameters. A more elegant and simple way to model erosion is to directly incorporate experimental kinetics laws into the mathematical model. We then develop a second model that is denoted *continuous dispersive analytical model*. The equations that govern the evolution of the mass density distribution due to the erosion is based on the kinetics law defined by Kao and Mason or Powell and Mason or Rwei et al,... According to this approach, we define four models respectively denoted pointwise, surface, volume and energetical model. Each of these models only depends on one parameter κ. This parameter can be easily determined by experiments and corresponds to the parameter that appears in relevant kinetics laws. With these models, only one calculation is needed to obtain the evolution of the mass density distribution at any time step if the value of κ does not vary with time.

The evolution of a given mass density distribution in a prescribed flow is different with each continuous model because they depend on different kinetics laws. The decrease in agglomerates size and the amount of fragments generated by the erosion mechanism in a given time period depends on the model selected. In order to evaluate the quality of our model, we measure the evolution of a given mass density distribution of carbon black agglomerates in rubber when they are mixed in a Mooney rheomether. This experiment is performed at several shear rates and during different mixing times. The mass density distribution of the carbon black agglomerates in such a mix is obtained with the help of a specific optical device. The comparison between these experimental results and the numerical evolution of the mass density distribution in the same flow condition shows that our models are able to predict the complex dynamics of the mass density distribution. Unfortunately, the value of the parameter κ extracted from the experiments performed by the Cemef group on the dispersion of a single agglomerate in rubber matrix provides a too slow erosion. The mechanism of rupture and erosion can occur simultaneously in the Mooney rheometer and it is not the case in the Cemef experiments. Moreover, the mass concentration of carbon black in the rubber matrix is high and each agglomerate interacts with its neighborhood. Collision between agglomerates can then be observed. All these perturbations increase the speed of the dispersion mechanism and might explain the deviation observed between the numerical and experimental results with this value of κ. But, we also show that a good agreement between experimental and numerical results can be obtained with each model if we give the relevant value at the parameter κ. Obviously, the quality of the results depends on the model considered and we observe that the volume model is the most efficient. In this model, the dispersion mechanism is modeled as a mechanism at the boundary between erosion and rupture. Finally, we can remark that these models are a good compromise between simplicity and physical reality.

The mixing efficiency of two kinds of rotor called *ZZ2 rotor* and *Old-Standard rotor* have been evaluated. The flow pattern generated by each couple of rotor in the mixer chamber has been calculated with a constrained finite element formulation for non-conforming meshes. From this information, we calculate the trajectory of 500 particles randomly launched in the flow domain. Along each trajectory, we calculate the evolution of a given mass density distribution as a function of the shear rate with the volume model. The comparison of these results allows us to evaluate the dispersive mixing efficiency of both rotors. It appears that the ZZ2 and the Old-Standard rotors have approximately the same efficiency but the specific power consumption is the smallest with the Old-Standard rotor. At the same time, the study of the distribution of these particles in the flow domain show that the distribution of these particles is faster with the ZZ2 rotors than with the Old-Standard rotors.

Future developments

A lot of new research ways are still open. On one hand, it would be interesting to investigate in details why the information on the parameter κ of the kinetics law obtained by the Cemef group cannot be directly used in this work. For this, we could repeat the experiments performed in the Mooney rheometer at different levels of concentration of carbon black agglomerates to observe the effect of this parameter on the evolution of the mass density distribution. We could also study the protocol used to fix the sample rubber-carbon black mixed in the Mooney rheometer. If the mixing time to prepare this sample is long, the carbon black agglomerates could be impregnated by the matrix and this would modify their behavior with respect to the experiments carried out by the Cemef. On the other hand, we could focus on the study of the rupture mechanism by experimental and theoretical ways in order to determine information on the typical rupture time required to observe rupture and on the number of fragments generated by each rupture.

At the end of this thesis, we present a test case in which we evaluate the mixing efficiency of two kinds of rotor. In this simulation, we assume that the flow is isothermal and that the mixer chamber is fully filled. But, the mixing of rubber with carbon black agglomerates is a non-isothermal process and the mixer chamber is not fully filled except at the start of the mixing. Of course, these conditions affect the shear rate field and therefore the evolution of the mass density distribution during the mixing. It would be interesting to investigate the effect of both parameters on the dispersive mixing efficiency of this rotor. This would require the development of new techniques permitting the flow calculation in a partially field domain. The calculation of the non-isothermal flow in the mixer chambers seems less challenging but the increase in temperature due to the viscous heating in the clearance zones could lead to numerical issues.

List of Tables

List of Figures

Bibliography

[Alsteens et al,2003] Alsteens, B., Avalosse, Th., Marchand, Y., Slachmuylders, E.,*Effect of the full-slip condition along rotors on the mixing efficiency of internal mixers*,Proceedings. of the 62th Annual Conference of the Society of Plastic Eng. (ANTEC), p.173 (2003)

[Alsteens et al,2005] Alsteens, B., Legat, V., Avalosse, Th., *Parametric study of the mixing efficiency in a kneading block section of a twin-screw extruder*, International Polymer Processing Journal, Vol XIX, Issue 3, p.207 (2005).

[Astruc et al,2004] Astruc, M., Collin, V., Rusch, S., Navard, P., Peuvrel-Disdier, E., *Infiltration of uncured elastomers into silica agglomerates*, J. App. Polymer Sci., accepted in 2004.

[ASTM] *ASTM Test Method D1510*, American Society for Testing and Materials, Philadelphia.

[Avalosse et al,1996] Avalosse, Th., *Numerical Simulation of Distributive Mixing in 3-D Flows* ,Macromol. Symp. 112, p.91 (1996).

[Avalosse et al,1997] Avalosse, Th., Crochet, M., *Finite-Element Simulation of Mixing:1. Two-Dimensional Flow in Periodic Geometry*, AIChE J. 43 (3), p.577 (1997).

[Avalosse et al,2000] Avalosse, Th., Rubin, Y., *Analysis of Mixing in corotating twin-screw extruders through numerical simulation*, Intern. Polym. Processing 15(2) (2000).

[Bakalis et al,2002] Bakalis, S., Karwe, M.V., *Velocity distributions and volume flow rates in the nip and translational regions of a co-rotating, self-wiping, twin-screw extruder*, J. Food Eng. 51, p.273 (2002).

[Barnes et al,1989] Barnes, H.A., Hutton, J.F., Walters, K. : An Introduction to Rheology. Elsevier, Amsterdam (1989).

[Bertrand et al,2003] Bertrand, F., Thibault, F., Delamare, L., Tanguy, P.A., *Adaptive finite element simulations of fluid flow in twin-screw extruders*, Comput. Chem. Eng. 27, p.491 (2003).

[Berzin et al,2002] Berzin, F., Vergnes, B., *A theoretical approach to solid filler dispersion in a twin-screw extruder*, Polymer Engineering and Science, Vol. 42, No. 3 (2002).

[Bigio et al,1990] Bigio, D., Stry, W., Polym. Eng. Sci. 30, p.153 (1990).

[Bigio et al,1991] Bigio, D., Zerafati, S., Polym. Eng. Sc. 31, p.1400 (1991).

[Bird et al,1960] Bird, R.B., Steward, W.E., Lightfoot, E.N., *Transport Phenomena*, John Wiley ed., NY (1960).

[Bravo et al,2000] Bravo, V.L., Hrymak, A.N., Wright, J.D., *Numerical Simulation of Pressure and Velocity Profiles in Kneading Elements of a Co-Rotating Twin-Screw Extruder*, Polym. Eng. and Sc. 40(2), p.525 (2000).

[Bohin et al,1994] Bohin, F., Feke, D.L., Manas-Zloczower, I., *Penetration of silicone polymers onto silica agglomerates and its influence on dispersion mechanism*, Rubber Chem. Technol. 67, p.602 (1994)

[Bohin et al,1994] Bohin, F., Manas-Zloczower, I., Feke, D.L., *Study of silicone polymers penetration in silica agglomerates and its influence on dispersion mechanism*, Rubber Chem. Technol, 67, p. 602 (1994).

[Bohin et al,1996] Bohin, F., Manas-Zloczower, I., Feke, D.L., *Kinetics of dispersion for sparse agglomerates in simple shear flows: application to silica agglomerates in silicones polymers*, Chem. Eng. Sci. 51, No. 23, p.5193 (1996).

[Bolen et al,1958] Bolen, W.R., Colwell, R.E., *Intensive mixing*, Society of Plastics Engineering Journal, Vol. 14, No. 8, p.24 (1958).

[Booy et al,1978] Booy. M.L., *Geometry of Fully Wiped Twin-Screw Equipment*, Polym. Eng. Sc. 18(12), p.973 (1978).

[Booy,1980] Booy, M.L., *Isothermal Flow of Viscous Liquids in Corotating Twin Screw Devices*, Polym. Eng. Sc. 20 (18), p.1220 (1980).

[Brezzi et al,1991] Brezzi, F., Fortin, M. : Mixed and hybrid finite elements methods. Springer, New York (1991).

[Carneiro et al,2002] Carneiro, O.S., Poulesquen, A., Covas, J.A., Vergnes, B., Intern. Polym. Process. 17, p.301 (2002).

[Chandrasekaran et al,1997] Chandrasekaran, M., Marcroft, H., Bakalis, S., Karwe, M.V., *Applications of laser Doppler anemometry in understanding food processing operations*, Trends in Food Sc. Technol. 8, p.369 (1997).

[Cheng et al,1968] Cheng, D.C.-H., *The tensile strength of powders*, Chemical Engineering Science, 23, p.1405 (1968).

[Collin et al,2004] Collin, V., Peuvrel-Disdier, E., *In situ quantitative study of dispersion mechanism of carbon black clusters in an elastomer under shear.*, submitted to Macromolecule (2004)

[Collin,2004] Collin, V., *Etude rheo-optique des mécanismes de dispersion du noir de carbone dans des élatsomères.*, Thesis of the Ecole National Supérieur des Mines de Paris (2004).

[Cotten et al,1978] Cotten, G., Thiele, J.L., *Influence of carbon black on processability of rubber stock III. Extensional viscosity*, Rubber Chem. Technol, 51, p. 749 (1978).

[Cotten,1984] Cotten, G., *Mixing of carbon black with rubber: I. Measurement of dispersion rate by changes in mixing torque*, Rubber Chem. Technol, 57, p. 118 (1984).

[Danckwerts et al,1951] Danckwerts, P.V., *Theory of Mixtures and Mixing* ,Appl. Sc. Res. A3, p.279 (1951).

[Debbaut et al,1991] Debbaut, B., Keunings, R., Crochet, M.J., Proc. Europ. Conf. New Adv. Comput. Struct. Mech., p.689 (1991).

[Dizon et al,1976] Dizon, E.S., *Processing in an internal mixer as affected by carbon black properties*, Rubber Chemisstry and technology, Vol. 49, p.12 (1976).

[Freakley et al,1978] Freakley, P.K., Wan Idris, W.Y., *Visulization of flow during the processing of rubber in an internal mixer*, Rubber Chemical Technology, 52, p.134 (1978)

[Freakley et al,1987] Freakley, P.K., Patel, S.R., *Internal mixing : a practical investigation of the flow and temperature profiles during a mixing cycle.*, Rubber Chemical Technology, 58, p.751 (1987)

[Erdmenger et al,2001] Erdmenger, R., Chem. Ing. Tech., 36, p.175 (1964).

[Galaktionov et al,2001] Galaktionov, O.S., Anderson, P.D., Kruijt, P.G.M., Peters, G.W.M., Meijer, H.E.H., *A mapping appraoch for three-dimensional distributive mixing analysis*, Comput. Fluids 30, p.271 (2001).

[Grieffies,2004] Griffies, S.M., *Fundamentals of Ocean Climate Models*,Princeton University Press,2004.

[Gotsis et al,1989] Gotsis, D., Kaylon, D.M., SPE ANTEC Tech. Papers 35, p.44 (1989).

[Guth et al,1938] Guth, E., Gold, O., Phys. Rev., 53, p.322 (1938).

[Hardley et al,1985] Hardley, P.A., Parfitt, G.D., *Dispersion of powders in liquids. 1. The contribution of the van der Walls force to the cohesiveness of carbon black powders*, Langmuir, 1, p.651 (1985)

[Huang,1987] Huang, K., *Statistical Mechanics*, John Wiley and Sons, 1987.

[Ishikiwa et al,2000] Ishikiwa, T., Nagashima, Y., Funatsu, K., Polym. Eng. Sc. 40(2), p.357 (2000).

[Ishikiwa et al,2001] Ishikawa, T., Kihara, S., Funatsu, K., *3-D Non-Isothermal Flow Field Analysis and mixing Performance Evaluation of Kneading Blocks in a Corotating Twin screw Extruder*, Polym. Eng. Sc. 41(5), p.840 (2001).

[Leblanc,1996] Leblanc, J., *Rhéologie des élastomères et mise en oeuvre des polym ‘eres.*, Artel Publishers, Namur (1996).

[Li et al,1994] Li, Q., Manas-Zloczower, I., Feke, D.L., *Influence of aggregate and matrix infiltration on the dispersion behavior of carbon black agglomerates*, Rubber Chem. Technol., 68, p. 836 (1995).

[Lozano et al,2003] Lozano, T., Lafleur, P.G., Grmela, M., Vergnes, B., *Modeling filler dispersion along a twin-screw extruder*, Intern. Polymer Processing XVIII, p.12 (2003).

[Lozano et al,2002] Lozano, T., Lafleur, P.G., Grmela, M., Vergnes, B., Polym. Eng. Sci. 42, p.347 (2002).

[Kao et al,1975] Kao, S.V., Mason, S. G., *Dispersion of particles by shear*, Nature 253, p.619 (1975).

[Kendall et al,1988] Kendall, K., *Agglomerate strength*, Powder Metallurgy, 31(1), p.28 (1988).

[Kim et al,1994] Kim, P.J., White, J.L., Inter. Polym. Proc. IX, p.108 (1994).

[Macosko et al,1994] Macosko, C.W. : Rheology:principles, measurements, and applications. New York (1994).

[Manas et al,1985] Manas-Zloczower, I., Nir, A., Tadmor, Z., *Dispersive mixing in roll-mills*, Polymer Composites, Vol. 6, No. 4, p.222 (1985).

[Manas et al,1988] Manas-Zloczower, I., Feke, D.L., *Analysis of agglomerate separation in linear flow fields*, Intern. Polymer Processing II, p.3 (1988).

[Manas et al,1989] Manas-Zloczower, I., Feke, D.L., *Analysis of agglomerate rupture in linear flow fields*, Intern. Polymer Processing IV, p.3 (1989).

[Manas et al,1994] Manas-Zloczower, I., Tadmor, Z., *Mixing and Compounding of Polymers*, Hanser Publishers, Munich Vienna New York (1994).

[Manas et al] Manas-Zloczower, I., Nir, A., Tadmor, Z., *Dispersive mixing in internal mixers - A theoretical model based on agglomerate rupture*, Rubber Chemistry and Technology, Vol. 55, p.1250.

[Meijer,1997] Meijer, H.E.H. : Material Science and Technology, A comprehensive Treatment 18. Wiley Publishers (1997).

[Min et al,1985] Min, K., White, J.L., *Flow visualization of the motions of elastomers and molten plastics in an internal mixer*, Rubber Chemical Technology, 58, p.1024 (1985)

[Min et al,1987] Min, K., White, J.L., *Flow visualization investigations of the addition of carbon black and oil to elastomers in an internal mixer*, Rubber Chemical Technology, 60, p.361 (1987)

[Optigrade] http://www.techpro-usa.com/disper.htm

[Ottino et al,1989] Ottino J.M. : The Kinematics of mixing: stretching, chaos and transport. Cambridge university Press, Cambridge (1989).

[Pliskin et al,1972] Pliskin, I., Tokita, N., *Bound rubber in elastomers: Analysis of elastomer-filler interaction and its effect on viscosity and modulus of composite systems.* J. Appl. Polym. Sc., 16, p.473 (1972).

[Potente et al,1997] Potente, H., Flecke, J., *Analysis and Modeling of the Residence Time Distribution in Intermeshing Co-Rotating Twin-Screw Extruders Based on Finite Elements Simulations*, Proc. 55th Annu. Tech. Conf. SPE, p.110 (1997).

[Rios et al,2000] Rios, A.C., Osswald, T.A., *Comparative study of rhomboidal mixing sections using the boundary element method*, Eng. Analysis Boundary Element 24, p.89 (2000).

[Roberts,1994] Roberts, A.J., *A one-dimensional introduction to continuum mechanics*, World Scientific Publishing, Singapore New Jersey London Honk Kong (1994).

[Rumph,1962] Rumph, H., *Agglomeration*, W.A. Knepper ed., New-York (1962).

[Rwei et al,1990] Rwei, S.P., Manas-Zloczower, I., *Observation of carbon black agglomerate dispersion in simple shear flows*, Polymer Engineering and Science, Vol. 30, No. 12, p.701 (1990).

[Rwei et al,1991] Rwei, S.P., Manas-Zloczower, I., Feke, D.L., *Characterization of Agglomerate Dispersion by Erosion in Simple Shear Flows*, Polym. Eng. Sci. 31, No. 8, p.558 (1991).

[Rwei et al,1991] Rwei, S.P., Horwatt, S.W., Manas-Zloczower, I., Feke, D.L., *Observation and analysis of carbon black agglomerate dispersion in simple shear flows*, International Polymer Processing VI, p.98 (1991).

[Sastrohartono et al,1990] Sastrohartono, T., Esseghir, M., Kwon, T., Sernas, V., Polym. Eng. Sci. 30, p.1382 (1990).

[Scuratti et al,2002] Scuratti, Manas-Zloczower, I., *Model and analysis of kinetics erosion in simple shear flows*, Rubber Division Meeting, Georgia (2002).

[Seyvat et al,2001] Seyvet, O., Navard, P., *Collision-induced dispersion of agglomerate suspensions in a shear flows*, J. Appl. Polym. Sci. 78(5), p.1130 (2001).

[Shaffiqa et al,2000] Shaffiqa, J., Bravo, V.L., Wood, Ph., Hrymak, A.N., *Experimental Validation of Numerical Simulation of the Kneading Disc Section in a Twin Screw Extruder*, Polym. Eng. and Sc. 40(4), p.892 (2000).

[Smit et al,1970] Smit, P.P.A., Van Der Vegt, Kautsch., Gummi, Kunstst, 23(4), p.147 (1970).

[Smoluchowski et al,1917] Smoluchowski, M., *Versuch einer mathematischen theorie des koaguationskinetics kolloduider lösungen*,Z. phys. Chem., p.129 (1917).

[Soontag et al,1987] Soontag, R.C., Russel, W.B., *Structure and break-up of flocs subjected to fluid stresses II. Theory*, J. Colloid Interface Science, 113, p.399 (1987).

[Speur et al,1987] Speur, J.A., Mavridis, H., Vlachopoulos, J., Janssens L.P.B.M., Adv. Polym. Tech. 7, p.39 (1987).

[Stein et al,1969] Stein, F., *Particle size measurements with phase contrast microscopy*, Powder Technology, Volume 2, Issue 6, pp. 327-334 (1969).

[Szydlowski et al,1987] Szydlowski, W., Brzoskowski, R., White, J.L., Int. Polym. Process. 1, p.207 (1987).

[Tadmor et al,2001] Tadmor, Z., *Forces in dispersive mixing*, Industrial Engineering Chemical Fundamental, Vol. 15, p.346 (1976).

[Todd et al,1990] Todd, D.B., *Drag and Pressure Flow in Twin screw Extruder*, Inter. Polym. Proc. VI,p.143 (1991).

[Todd,1998] Todd, D.B. : Plastic Compounding Equipment and Processing, Hanser Publishers, Munich (1998).

[White et al,1974] White, J.L., Crowder, J.W., *The influence of carbon black on the extrusion characteristics and rheological properties of elastomers: Polybutadiene and butadiene-styrene copolymer*, J. Appl. Polym. Sc., 18, p.1013 (1974).

[White,1995] White, J.L., *Rubber Processing : Technology - Materials - Principles*, Hanser Publishers, Munich Vienna New York (1995).

[Yamada et al,1994] Yamada, H., Manas-Zloczower, I., Feke, D.L., *Influence of matrix infiltration on the dispersion kinetics of carbon black agglomerates*, Powder Technol., 92, p. 163 (1997).

[Yamada et al,1998] Yamada, H., Manas-Zloczower, I., Feke, D.L., *The influence of matrix viscosity and interfacial properties on the dispersion kinetics of carbon black agglomerates*, Rubber Chem. Technol., 71, p.1 (1998).

[Yoshinaga et al,2000] Yoshinaga, M., Katsuki, S., Miyazaki, M., Liu, L., Kihara, S., Funatsu, K., Polym. Eng. Sc. 40(1), p.168 (2000).